Complex Modes in Lossless Shielded Microstrip Lines

WEI-XU HUANG AND TATSUO ITOH, FELLOW, IEEE

Abstract — **Possible existence of complex modes is investigated in lossless shielded microstrip lines. The analysis is based on the singular integral equation approach, which provides good convergence properties. Accurate numerical results are obtained by using a 10×10 matrix equation.**

I. Introduction

Recently, a number of investigations of complex modes in lossless waveguiding structures have been reported [1]–[4]. The lossless shielded guide with a dielectric insert may or may not support complex modes, depending on the structural parameters and the frequency range. It has been shown that even though the complex modes are not strongly excited, they greatly affect the modal energy distribution at both sides of the discontinuity. Hence, in the millimeter-wave device design, the analysis of complex modes is of great importance.

In Section II of this paper, a brief review of the singular integral equation method is presented for formulation of the problem of the shielded microstrip line (Fig. 1). Since the details are given in [5], only the key steps are provided. In the singular integral equation approach, the singular behavior at the edges of the strip is incorporated so that the convergence is accelerated. Instead of a large matrix in many other methods, only a small matrix needs to be treated in the singular integral equation approach.

In Section III, the method is used for the analysis of three lossless shielded microstrip line structures with different permittivities in the substrate. To confirm the validity of the method, results are compared with existing data for propagating modes [6]. The complex modes have been found in the moderate and high permittivity structures.

II. Formulation

The cross section of the lossless shielded microstrip line is shown in Fig. 1. The structure consists of a conducting strip placed on a dielectric substrate. The TM and TE field components in regions 1 and 2 can be derived from the scalar potentials $\psi_i^{(e)}$ and $\psi_i^{(h)}$, the subscript $i=1,2$ designating the region 1 or 2. The scalar potentials satisfy the two-dimensional Helmholtz equations as well as the requirements that the tangential electric fields vanish on the waveguide and that the tangential magnetic fields vanish on the plane of symmetry $x=0$. It is appropriate to write

$$\psi_1^{(e)} = \sum_{n=1}^{\infty} A_n^{(e)} \sinh \alpha_n^{(1)} y \cos \hat{k}_n x \tag{1a}$$

$$\psi_2^{(e)} = \sum_{n=1}^{\infty} B_n^{(e)} \sinh \alpha_n^{(2)} (h-y) \cos \hat{k}_n x \tag{1b}$$

$$\psi_1^{(h)} = \sum_{n=1}^{\infty} A_n^{(h)} \cosh \alpha_n^{(1)} y \sin \hat{k}_n x \tag{1c}$$

Manuscript received May 21, 1987; revised August 14, 1987 This work was supported in part by the Office of Naval Research under Contract N00014-79-0553, by the Army Research Office under Contract DAAG 29-84-K-0076, and by the Air Force under Contract AFOSR-86-0036

The authors are with the Department of Electrical and Computer Engineering, University of Texas at Austin, Austin, TX 78712

IEEE Log Number 8717579

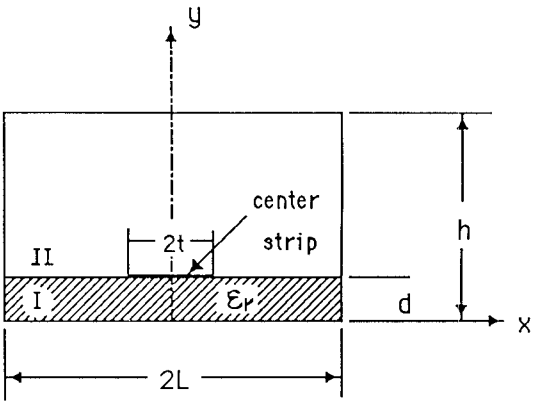

Fig. 1. Cross section of shielded microstrip line.

$$\psi_2^{(h)} = \sum_{n=1}^{\infty} B_n^{(h)} \cosh \alpha_n^{(2)} (h-y) \sin \hat{k}_n x \tag{1d}$$

$$\alpha_n^{(1)} = \sqrt{\hat{k}_n^2 + \beta^2 - \epsilon_r k_0^2} \qquad \alpha_n^{(2)} = \sqrt{\hat{k}_n^2 + \beta^2 - k_0^2}$$

where $\hat{k}_n = (n-1/2)\pi/L$ and $k_0 = \omega\sqrt{\epsilon_0 \mu}$, the free-space wavenumber. β is the propagation constant, and the superscripts (e) and (h) are associated with E(TM) and H(TE) fields, respectively. ϵ_0 and μ are the permittivity and permeability of vacuum and ϵ_r is the relative dielectric constant of the substrate.

By applying the continuity condition and the boundary condition equations on the superposed TE,TM hybrid fields and transforming these boundary condition equations into an auxiliary set of equations [5], an infinite set of equations is obtained:

$$\sum_{m=1}^{\infty} a_{mp} \bar{A}_m^{(e)} + \sum_{n=1}^{\infty} b_{np} \bar{A}_n^{(h)} = 0 \qquad p=1,2,\cdots \tag{2a}$$

$$\sum_{m=1}^{\infty} c_{mq} \bar{A}_m^{(e)} + \sum_{n=1}^{\infty} d_{nq} \bar{A}_n^{(h)} = 0 \qquad q=1,2,\cdots \tag{2b}$$

where a_m, b_m, c_m, d_m (see [5]) have the property that they decrease extremely rapidly with an increasing value of m, so that the associated matrix can be truncated to a relatively small size.

The solution of the determinant of (2) equated to zero yields the desired value β:

$$\det[A] = 0. \tag{3}$$

The elements of the matrix $[A]$, a_m, b_m, c_m, and d_m, depend on the unknown propagation constant β. If only the real β^2 is assumed, no complex modes can be found. During the search for the eigenvalue β^2 on the real axis, the real solution for β^2 may disappear. Hence the zeros of $\det[A]$ must be looked for in the complex plane rather than on the real axis of β^2. The complex β will be found if complex modes exist.

III. Results and Analysis

A. Higher Order Modes and Convergence

The roots of the characteristic equation for the propagation constant β can be calculated from (3). The propagation constant β depends on the structural and operating parameters of the shielded microstrip line. As expected, the number of higher order propagating modes increases with an increasing frequency.

0018-9480/88/0100-0163$01.00 ©1988 IEEE

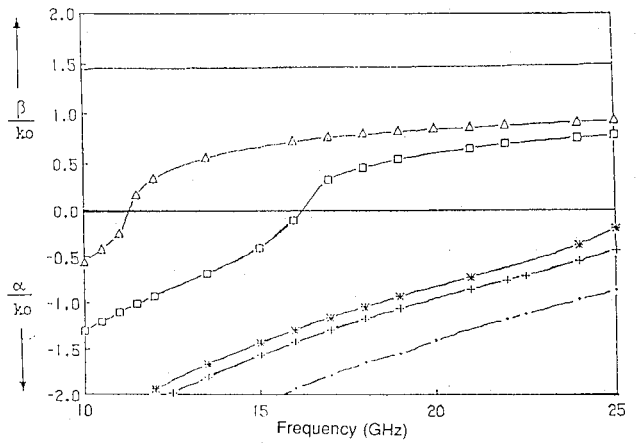

Fig. 2. Propagation constant $\gamma = \alpha + j\beta$ normalized with $k_0 = \sqrt{\epsilon_0 \mu_0}$ versus frequency. Parameters: $\epsilon_r = 2.65$, $L = 6.35$ mm, $t = 0.635$ mm, $d = 1.27$ mm, $h = 12.7$ mm.

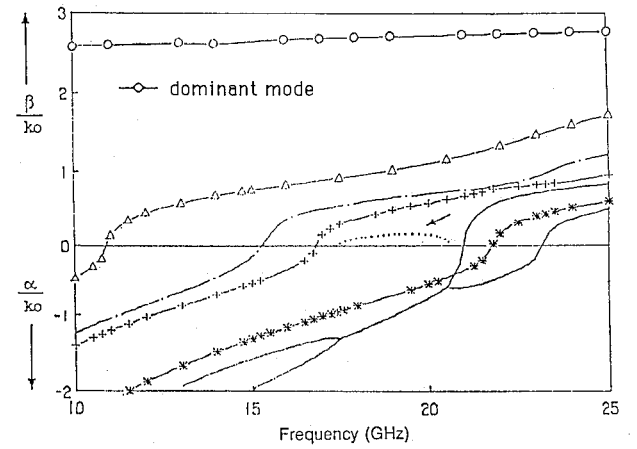

Fig. 3. Propagation constant $\gamma = \alpha + j\beta$ normalized with $k_0 = \sqrt{\epsilon_0 \mu_0}$ versus frequency. Parameters: $\epsilon_r = 8.875$, $L = 6.35$ mm, $t = 0.635$ mm, $d = 1.27$ mm, $h = 12.7$ mm.

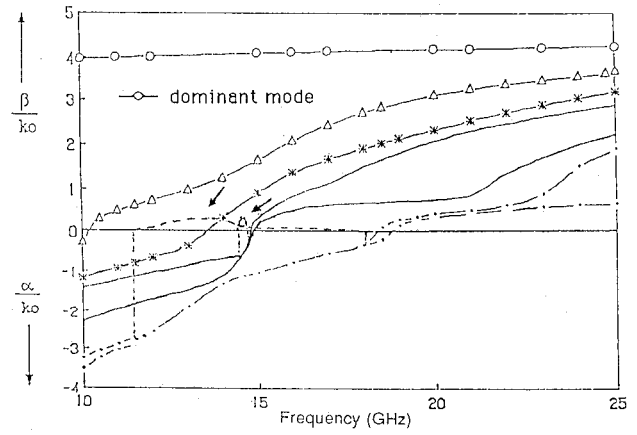

Fig. 4. Propagation constant $\gamma = \alpha + j\beta$ normalized with $k_0 = \sqrt{\epsilon_0 \mu_0}$ versus frequency. Parameters: $\epsilon_r = 20$, $L = 6.35$ mm, $t = 0.635$ mm, $d = 1.27$ mm, $h = 12.7$ mm.

Figs. 2, 3, and 4 show the normalized propagation constant $\gamma/k_0 = \alpha/k_0 + j\beta/k_0$ versus frequency. In the nonpropagating range, $\gamma/k_0 = \alpha/k_0$ is plotted in the opposite direction.

By choosing a 10×10 matrix equation, the first five higher order modes in addition to the dominant mode have been obtained. In the propagating range ($\beta > 0$, above cutoff), the dispersion characteristics have been compared with Yamashita's results [6] for the same structural parameters (see Fig. 3). The results calculated by the two different methods are indistinguishable (shown in the same lines). The accuracy of eigenvalue β has been checked by increasing the matrix size to 12×12, and is found that the error is below 0.1 percent. Comparison of the results by the two matrix sizes is given in Table I for 20 GHz. From this comparison, it is concluded that the 10×10 matrix is large enough for accurate eigenvalue calculation.

TABLE I
PROPAGATION CONSTANT OF SIX MODES FOR THE TWO DIFFERENT MATRICES

Matrix	Mode 1	Mode 2	Mode 3	Mode 4	Mode 5	Mode 6
10×10	(2.7089,0.)	(1.1029,0.)	(0.70499,0.)	(0.59408,0.)	(0.,0.55270)	(0.15350,0.77168)
12×12	(2.7086,0.)	(1.1031,0.)	(0.72499,0.)	(0.59418,0.)	(0.,0.55274)	(0.15345,0.77162)

Structure parameters: same as Fig. 2.

B. Complex Modes and Mode Conversion

For a low permittivity ($\epsilon_r = 2.65$, Fig. 2), an ordinary dispersion behavior is obtained, and no complex modes have been found. For a moderately high permittivity ($\epsilon_r = 8.875$, Fig. 3), however, between 17.6 GHz and 20.6 GHz indicated by the dashed curve, the eigenvalue solution leads to complex propagation constants $\gamma = \alpha \pm j\beta$, in spite of the assumption that the shielded microstrip line is lossless. The complex conjugate pair has a physical meaning. Each of the modes in the pair propagates in the opposite directions along the axis. However, the total power transmitted by the pair of complex waves is zero.

With a high permittivity ($\epsilon_r = 20$, Fig. 4), complex modes are also found in the two ranges, 11.6 GHz–17.75 GHz and 14.45 GHz–14.77 GHz indicated by the dashed curve.

The mode conversion occurs when the frequency is changed. As the frequency is decreased, the evanescent modes degenerate into a pair of complex waves propagating in the $+z$ and $-z$ directions with $j\beta$, and the attenuation constant is α. For a still lower frequency, the complex modes split into two evanescent modes. In Fig. 3, complex modes exist only in a certain frequency range. For different structural parameters, such as a different dielectric permittivity ϵ_r, complex modes may or may not exist. At a low ϵ_r in Fig. 2, no complex modes have been found. In summary, the evanescent modes become complex modes within one or more ranges of certain structural parameters (e.g., the permittivity ϵ_r) at a given frequency or, alternatively, within one or more frequency ranges at given structural parameters.

IV. CONCLUSIONS

An analysis of the guided modes in a lossless shielded microstrip line has been presented as to the possible existence of complex modes. The analysis is based on the singular integral equation method. By means of this method, propagation constants of the higher order modes (including complex modes) have been calculated. Complex modes exist only in a certain frequency range. At a certain frequency, two evanescent modes are transformed to a pair of complex modes. As the frequency is increased (or decreased), the pair of complex modes split and return to two evanescent modes. These phenomena are the same as those in finlines and shielded dielectric image guides reported recently [1]–[4].

We need to mention here that we reported the existence of complex modes at the given structural parameters and frequencies. Before a more general statement on the conditions for existence of complex modes is made, it is necessary to perform more extensive numerical calculations on a number of structures

with differential structural parameters. An alternative approach would be to find the field distributions of these complex modes so that physical insight can be gained for their existence. These efforts are planned in the near future.

REFERENCES

[1] A. S. Omar and K. Schunemann, "Effect of complex modes on finline discontinuities," in *IEEE MTT-S Dig.*, 1986, pp. 123–126.

[2] A. S. Omar and K. Schunemann, "New type of evanescent modes in fin-lines," in *Proc. European Microwave Conf.*, 1985, pp. 317–322.

[3] A. S. Omar and K. Schunemann, "Formulation of the singular integral equation technique for planar transmission lines," *IEEE Trans. Microwave Theory Tech.*, vol. MTT-33, pp. 1313–1321, Dec. 1985

[4] J. Strube and F. Arndt, "Rigorous hybrid-mode analysis of the transition from rectangular waveguide to shielded dielectric image guide," *IEEE Trans. Microwave Theory Tech.*, vol. MTT-33, pp. 391–401, May 1985

[5] R. Mittra and T. Itoh, "A new technique for the analysis of the dispersion characteristics of microstrip lines," *IEEE Trans. Microwave Theory Tech.*, vol. MTT-19, pp. 47–56, Jan. 1971.

[6] E. Yamashita and K. Atsuki, "Analysis of microstrip-like transmission lines by nonuniform discretization of integral equations," *IEEE Trans. Microwave Theory Tech.*, vol. MTT-24, pp. 195–200, Apr. 1976.

[7] S. B. Rayevskiy, "Some properties of complex waves in a double-layer circular, shielded waveguide," *Radio Eng. Electron. Phys.*, vol. 21, pp. 36–39, 1976.

[8] V. A. Kalmyk, S. B. Rayevskiy, and V. P. Ygryumov, "An experimental verification of existence of complex waves in a two-layer, circular, shielded waveguide," *Radio Eng. Electron. Phys.*, vol. 23, pp. 17–19, 1978.

[9] U. Crombach, "Complex waves on shielded lossless rectangular dielectric image guide," *Electron. Lett.*, vol. 19, no. 14, pp. 557–558, July 1983